Available online at www.sciencedirect.com

Journal of Organometallic Chemistry 680 (2003) 212–217

Journal of Organometallic Chemistry

www.elsevier.com/locate/jorganchem

Functionalization of the macropolyhedral borate anion cluster $[B_{22}H_{22}]^{2-}$: isolation and characterization of the OH and OEt derivatives

O. Volkov [1], N.P. Rath, L. Barton *

Department of Chemistry and Biochemistry, and the Center for Molecular Electronics, University of Missouri-St. Louis, 8001 Natural Bridge Road, St. Louis, MO 63121, USA

Received 4 March 2003; received in revised form 24 April 2003; accepted 24 April 2003

Dedicated to Professor M.F. Hawthorne in celebration of his 75th birthday and a career of seminal contributions to polyhedral borane chemistry

Abstract

Preparation and characterization of the first derivatives of the fused macropolyhedral anion $[B_{22}H_{22}]^{2-}$ are reported. The species $[B_{22}H_{21}OH]^{2-}$ (**1**) and $[B_{22}H_{21}OEt]^{2-}$ (**2**) are obtained from workup of the products of the reaction between $HgBr_2$ and $[NBzlEt_3]_2[B_{22}H_{22}]$; a cluster involving the conjoining of a *closo*-B_{12} icosahedron with a *nido*-B_{10} cluster. Washing the products with ethanol followed by thin-layer chromatography allows the isolation of **1** and **2**, reproducibly, in yields of 27 and 20%, respectively. The species were characterized by NMR spectroscopy, elemental analysis and X-ray diffraction studies. The crystal structure determinations of the two species identify novel features. Apparently the influence of the O atoms in the ions $[B_{22}H_{21}OH]^{2-}$ and $[B_{22}H_{21}OEt]^{2-}$ results in the lengthening of what was a gunwale B–B connection adjacent to the junction of the two cages such that the distances are 2.180 and 2.230 Å, respectively. These latter are longer than the corresponding distance in the parent species $[B_{22}H_{22}]^{2-}$, which is 2.09 Å; quite long for a normal B–B distance. Thus it is assumed that these B atoms, in **1** and **2**, one of which bears the substituent, are not bonded to each other.

Keywords: Boranes; Boron hydrides; Macropolyhedral borane clusters; NMR spectroscopy; X-ray diffraction

1. Introduction

A major goal in modern borane cluster chemistry is the preparation of systems containing large numbers of boron atoms [1]. This interest is stimulated by efforts to emulate the success of fullerene chemistry [1,2] but more important to prepare systems for application in boron neutron capture therapy [3], and in materials chemistry [2,4]. The pioneer in all of these areas is Fred Hawthorne to whom this paper is dedicated [1e,2,3a,3d,3e]. In all this chemistry, the larger the number of boron atoms in the molecule the better. For many years the most readily accessible of the larger borane species were the $[B_{12}H_{12}]^{2-}$ anion [5], the isomeric pair of octadecaboranes [6], and the $[B_{20}H_{18}]^{2-}$ anion reviewed recently by Hawthorne [1e]. Typical studies in these general areas have involved the construction of large molecules through cluster fusion [1b,1c,1d,7,8], or linkage processes [1b] [9], and also the functionalization of the icosahedral B_{12}- and C_2B_{10}-*closo*-systems in order to provide useful lipophilic and hydrophilic materials for medical applications [10]. Although borate anions containing 24 [11,12] and 48 [12] boron atoms have been reported, currently the largest synthetic all-boron cluster for which a complete structural characterization is available is the anionic fused species $[B_{22}H_{22}]^{2-}$, recently reported almost simultaneously by two groups [7]. Now, we report the formation and characterization of the first derivatives of this potentially most useful system.

---

* Corresponding author. Tel.: +1-314-526-5334; fax: +1-314-515-5342.

E-mail address: lbarton@umsl.edu (L. Barton).

[1] Permanent address: Institute of Inorganic Chemistry, Russian Academy of Sciences, 630090 Novosibirsk, Russia.

0022-328X/03/$ - see front matter © 2003 Elsevier Science B.V. All rights reserved.
doi:10.1016/S0022-328X(03)00350-4

2. Experimental

Solvents used were reagent grade and were dried before use. The reaction was carried out using a Schlenk line and standard techniques for handling air-sensitive compounds. $[NBzlEt_3]_2[B_{22}H_{22}]$ was prepared according to the literature method [7b]. NMR spectroscopy (CD_3CN, 25 °C) was carried out on a Bruker ARX 500 spectrometer operating at 500.1 MHz for proton and 160.5 MHz for ^{11}B. Chemical shifts are reported in ppm to low field (high frequency) of $Et_2O \cdot BF_3$ for ^{11}B and of $SiMe_4$ for ^1H. Elemental analyses were done by Atlantic Microlabs, Inc., Norcross, GA.

3. Reaction of $[NBzlEt_3]_2[B_{22}H_{22}]$ with $HgBr_2$

A sample of $HgBr_2$ (210 mg, 0.58 mmol) was added under nitrogen to a solution of $[NBzlEt_3]_2[B_{22}H_{22}]$ (95 mg, 0.15 mmol) in 30 ml CH_2Cl_2 and stirred at room temperature for 6 days. Then, the reaction mixture was filtered over silica gel and 20 ml of EtOH was added to the yellow solution. Evaporation of CH_2Cl_2 resulted in the formation of a yellow residue. This was dissolved in the minimum amount of CH_2Cl_2 and applied to a TLC plate. The plate was developed using CH_2Cl_2/CH_3CN (8:1) as the mobile phase. Two boron-containing compounds were separated and identified as $[NBzlEt_3]_2[B_{22}H_{21}OH]$ (**1**, 23 mg, 0.04 mmol; 27%) and $[NBzlEt_3]_2[B_{22}H_{21}OEt]$ (**2**, 21 mg, 0.03 mmol; 20%). NMR spectra for $[NBzlEt_3]_2[B_{22}H_{21}OH]$ (**1**); ^{11}B: δ 25.2 (s, 1B), 13.6 (d, J(H/B) = 142 Hz, 1B), 11.3 (d, J(H/B) = 139 Hz, 1B), 1.8 (d, J(H/B) = 132 Hz, 1B), 0.8 (d, J(H/B) = 149 Hz, 1B), −2.8 (d, J(H/B) = 137 Hz, 1B), −3.2 (d, J(H/B) = 128 Hz, 1B), −8.4 (br, d, 3B), −10.5 (d, J(H/B) = 138 Hz, 1B), −11.4 (d, J(H/B) = 131 Hz, 2B), −13.6 (d, J(H/B) = 130 Hz, 1B), −15.5 (d, J(H/B) = 134 Hz, 2B), −16.7 (d, J(H/B) = 137 Hz, 1B), −20.0 (d, J(H/B) = 131 Hz, 1B), −24.1 (s, 1B), −27.5 (s, 1B), −31.2 (d, J(H/B) = 149 Hz, 1B), −32.8 (d, J(H/B) = 152 Hz, 1B). ^1H: δ 7.58−7.42 (m, 10H; C_6H_5), 4.32 (s, 4H; $CH_2C_6H_5$), 3.19 (q, J(H/H) = 7 Hz, 12H; CH_2CH_3), 1.35 (t, J(H/H) = 7 Hz, 18H; CH_2CH_3). Additional $^1H\{^{11}B\}$: δ 3.74 (2H, BH), 3.49 (2H, BH), 2.33 (2H, BH), 2.28 (2H, BH), 1.74 (1H, BH), 1.61 (3H, BH), 1.58 (2H, BH), 1.51 (1H, BH), 1.33 (1H, BH), 0.44 (1H, BH), −0.03 (2H, BH), −2.65 (1H, μ-H), −2.78 (1H, μ-H). NMR spectra for $[NBzlEt_3]_2[B_{22}H_{21}OEt]$ (**2**) ^{11}B: δ 28.5 (s, 1B), 13.2 (d, J(H/B) = 123 Hz, 1B), 12.4 (d, J(H/B) = 137 Hz, 1B), 2.3 (d, J(H/B) = 125 Hz, 1B), −2.7 (br, d, 1B), −3.3 (br, d, 1B), −3.8 (d, J(H/B) = 132 Hz, 1B), −8.1 (d, J(H/B) = 117 Hz, 1B), −9.2 (d, J(H/B) = 138 Hz, 2B), −10.9 (d, J(H/B) = 140 Hz, 1B), −11.7 (d, J(H/B) = 124 Hz, 1B), −12.2 (d, J(H/B) = 126 Hz, 1B), −13.0 (d, J(H/B) = 129 Hz, 1B), −14.6 (d, J(H/B) = 131 Hz, 1B), −17.5 (d, J(H/B) = 130 Hz, 2B), −19.4 (d, J(H/B) = 127 Hz, 1B), −23.7 (s, 1B), −27.6 (s, 1B), −29.8 (d, J(H/B) = 147 Hz, 1B), −32.8 (d, J(H/B) = 147 Hz, 1B). ^1H: δ 7.57−7.42 (m, 10H; C_6H_5), 4.32 (s, 4H; $CH_2C_6H_5$), 3.75 (br, 2H; OCH_2CH_3), 3.17 (q, J(H/H) = 7 Hz, 12H; CH_2CH_3), 1.35 (t, J(H/H) = 7 Hz, 18H; CH_2CH_3) 1.09 (t, J(H/H) = 7 Hz, 3H; OCH_2CH_3). Additional $^1H\{^{11}B\}$: δ 3.70 (2H, BH), 3.27 (2H, BH), 1.55 (1H, BH), 1.49 (2H, BH), 1.44 (3H, BH), 1.25 (1H, BH), 1.22 (2H, BH), 1.19(2H, BH), 1.02 (1H, BH), 0.38 (1H, BH), −0.01 (2H, BH), −2.48 (1H, μ-H), −2.87 (1H, μ-H).

The crystals of $[(\eta^5\text{-}C_5H_5)Fe(\eta^5\text{-}C_5H_4CH_2(Me)_3N)]_2[B_{22}H_{21}OH] \cdot EtOH$ (**3**) and $[(\eta^5\text{-}C_5H_5)Fe(\eta^5\text{-}C_5H_4CH_2(Me)_3N)]_2[B_{22}H_{21}OEt]$ (**4**) were obtained when the solvents were slowly evaporated from the CH_2Cl_2/EtOH solutions, containing excess of $[(\eta^5\text{-}C_5H_5)Fe(\eta^5\text{-}C_5H_4CH_2(Me)_3N)]I$, and $[NBzlEt_3]_2[B_{22}H_{21}OH]$ (**1**) or $[NBzlEt_3]_2[B_{22}H_{21}OEt]$ (**2**). Anal. Calc. for $[(\eta^5\text{-}C_5H_5)Fe(\eta^5\text{-}C_5H_4CH_2(Me)_3N)]_2[B_{22}H_{21}OH] \cdot EtOH$: C, 42.98; H, 8.18. Found: C, 43.43; H, 7.39%. Anal. Calc. for $[(\eta^5\text{-}C_5H_5)Fe(\eta^5\text{-}C_5H_4CH_2(Me)_3N)]_2[B_{22}H_{21}OEt]$: C, 43.92; H, 8.11. Found: C, 44.16; H, 8.05%. Single crystals of $[(\eta^5\text{-}C_5H_5)Fe(\eta^5\text{-}C_5H_4CH_2(Me)_3N)]_2[B_{22}H_{21}OH]$ were obtained by layering a CH_2Cl_2 solution with Et_2O and single crystals of $[(\eta^5\text{-}C_5H_5)Fe(\eta^5\text{-}C_5H_4CH_2(Me)_3N)]_2[B_{22}H_{21}OEt]$ were grown by slow diffusion of EtOH into a CH_2Cl_2 solution.

4. X-ray structure determinations

Single crystals with appropriate dimensions were mounted on glass fibers in random orientation. Preliminary examination and data collection were performed using a Bruker SMART Charge Coupled Device (CCD) Detector single crystal X-ray diffractometer using graphite monochromated Mo–Kα radiation ($\lambda = 0.71073$ Å) equipped with a sealed tube X-ray source. Preliminary unit cell constants were determined with a set of 45 narrow frames (0.3° in ϖ) scans. Data collection consisted of 3636 frames of intensity data collected with a frame width of 0.3° in ϖ and counting time of 15–30 s per frame at a crystal to detector distance of 4.950 cm. The double pass method of scanning was used to exclude any noise. The collected frames were integrated using an orientation matrix determined from the narrow frame scans. SMART and SAINT software packages [13] were used for data collection and data integration. Analysis of the integrated data did not show any decay. Final cell constants were determined by global refinement of the *xyz* centroids of thresholded reflections from the complete data set. Collected data were corrected for systematic errors using SADABS [14] based on the Laue symmetry using equivalent reflections. Crystal data and intensity data collection parameters are listed in Table 1. Struc-

Table 1
Crystal data and structure refinement for $[(\eta^5\text{-}C_5H_5)Fe(\eta^5\text{-}C_5H_4CH_2(Me)_3N)]_2[B_{22}H_{21}OH]\cdot 2CH_2Cl_2$ (**3**) and $[(\eta^5\text{-}C_5H_5)Fe(\eta^5\text{-}C_5H_4CH_2(Me)_3N)]_2[B_{22}H_{21}OEt]$ (**4**)

	3	4
Empirical formula	$C_{30}H_{66}B_{22}Cl_4Fe_2N_2O$	$C_{30}H_{66}B_{22}Fe_2N_2O$
Formula weight	962.17	820.37
Temperature (K)	120(2)	120(2)
Wavelength (Å)	0.71073	0.71073
Crystal system	monoclinic	triclinic
Space group	$P2(1)/c$	$P\bar{1}$
α (Å)	17.0264(4)	10.9209(14)
β (Å)	10.7867(2)	15.0656(19)
χ (Å)	27.4461(6)	15.891(2)
α (°)	90	113.668(9)
β (°)	102.8480(10)	96.283(10)
γ (°)	90	104.643(9)
V (Å^{-3})	4914.51(18)	2250.2(5)
Z	4	2
D_{calc} (Mg m^{-3})	1.300	1.211
Absorption coefficient (mm^{-1})	0.838	0.674
Crystal size (mm^3)	0.34 × 0.22 × 0.18	0.23 × 0.20 × 0.18
F(0 0 0)	1992	860
θ range for data collection (°)	1.52 to 26.00	1.58 to 27.50
Index ranges	$-21=h=20$, $-13=k=13$, $-33=l=33$	$-14=h=14$, $-19=k=17$, $-20=l=20$
Reflections collected	72518	54807
Independent reflections	9649 [$R_{int}=0.0972$]	10212 [$R_{int}=0.09$]
Max/min transmission	0.8638 and 0.7637	0.8883 and 0.8604
Data/restraints/parameters	9649/0/550	10212/0/596
Goodness-of-fit on F^2	1.028	1.010
Final R indices [$I>2\sigma(I)$] R_1	0.0831	0.0621
$wR2$ (all data)	0.2548	0.1572
Largest difference peak and hole (e Å^{-3})	0.731 and −0.586	0.510 and −0.449

ture solutions and refinement were carried out using the SHELXTL-PLUS software package [15]. The structures were solved by direct methods and refined successfully in the monoclinic space group $P2_1/c$ and triclinic space group $P\bar{1}$ for **3** and **4**, respectively. Full matrix least-squares refinement was carried out by minimizing $\Sigma w(F_o^2-F_c^2)^2$. The non-hydrogen atoms were refined anisotropically to convergence. The cage H's were located in both cases, however, the H atoms were refined only for **3**. All other hydrogen atoms were treated using an appropriate riding model (AFIX m3). The final structure refinement parameters are listed in Table 1. CH_2Cl_2 was found in the lattice of compound **3**. Complete listings of positional and isotropic displacement coefficients for hydrogen atoms, anisotropic displacement coefficients for the non-hydrogen atoms are deposited as supplementary material. Tables of calculated and observed structure factors are available in electronic format. Selected bond distances and angles are found in Table 2.

5. Results and discussion

Our initial attempts to effect $HgBr_2$-promoted coupling of $[B_{22}H_{22}]^{2-}$, analogous to the formation of $B_{18}H_{22}$ from $[B_9H_{12}]^-$ and $HgBr_2$ [16], were unsuccessful. This was not altogether surprising since other attempts to carry out this latter reaction led to the formation of $[B_9H_{12}Br_2]^-$ as the major product [17]. However, treatment of $[NBzlEt_3]_2[B_{22}H_{22}]$ with excess $HgBr_2$ under N_2 at ambient temperature, followed by stirring for 6 days, allowed the isolation of $[NBzlEt_3]_2[B_{22}H_{21}OH]$ (**1**) and $[NBzlEt_3]_2[B_{22}H_{21}OEt]$ (**2**), in 27 and 20% yields, respectively, after filtering over silica gel and treatment with ethanol. Presumably the silica gel, or water adsorbed on it, was the source of the OH moiety and the ethanol the source of the OEt moiety. These results were reproducible and we presume that the compounds are formed either by initial bromination followed by hydrolysis and alcoholysis of the B–Br bond or possibly via an intermediate with a B–Hg bond, which is reactive towards EtOH and H_2O. Intermediates were not isolated. Both **1** and **2** were characterized by ^{11}B and ^1H NMR spectroscopy; each exhibiting spectra with resonances accounting for 22 boron atoms and 21 cage-bonded H atoms. The spectra for **1** and **2** are more complex than that of the parent $[B_{22}H_{22}]^{2-}$ anion due to the absence of a mirror plane. Thus, the number of signals increased from 13 in the parent to 17 for **1** and 20 for **2**. In the ^{11}B NMR spectra of both **1** and **2**, three signals are singlets, and the others are doublets. The low-field singlets, at 25.2 and 28.5 ppm for **1** and **2**, respectively, correspond to the B atoms bearing the OH- and OEt-substituents. These are shifted to low field by 16.4 ppm for **1** and 19.4 ppm for **2**, relative to the unsubstituted $[B_{22}H_{22}]^{2-}$ cluster. The pairs of high-field singlets, at −24.1 and −27.5 ppm for **1** and −23.7 and −27.6 ppm for **2**, correspond to B(1,2); the naked boron atoms at the conjunction of the two clusters. These fall at −29.0 ppm in the parent $[B_{22}H_{22}]^{2-}$ [7b]. All other B atoms bear terminal H atoms and thus are observed as doublets. For each species, the two bridging H atoms were observed in the expected region −2.4–2.9 ppm. Attempts to perform 2D ^{11}B–^{11}B COSY experiments were unsuccessful due to a combination of intensity and instrumentation problems. Negative ion mass spectra showed molecular ion envelopes in the expected regions for **1** and **2** but comparison with calculated values was not possible because of substantial fragment overlap from the loss of more than one hydrogen atom. The presence of envelopes centered in the expected regions, m/z 276 for **1** and 304 for **2**, support the formulation of the two species and elemental analysis of the $[(\eta^5\text{-}C_5H_5)Fe(\eta^5\text{-}C_5H_4CH_2(Me)_3N)]^+$ salts **3** and **4** was quite satisfactory.

Table 2
Bond angles and distances for $[(\eta^5\text{-}C_5H_5)Fe(\eta^5\text{-}C_5H_4CH_2(Me)_3N)]_2[B_{22}H_{21}OH]$ (**3**) and $[(\eta^5\text{-}C_5H_5)Fe(\eta^5\text{-}C_5H_4CH_2(Me)_3N)]_2[B_{22}H_{21}OEt]$ (**4**)

	(**3**)	(**4**)		(**3**)	(**4**)
Bond length					
O(1)–B(4′) (**3**)	1.383(8)		B(1′)–B(6′)	1.752(12)	1.810(7)
O(1)–B(5′) (**4**)		1.402(5)	B(2′)–B(3′)	1.747(13)	1.751(7)
O(1)–H(1A) (**3**)	0.8400		B(2′)–B(6′)	1.678(14)	1.757(6)
O(1)–C(1′) (**4**)		1.448(4)	B(3′)–B(8′)	1.734(12)	1.731(6)
B(1)–B(2)	1.758(11)	1.758(5)	B(3′)–B(7′)	1.789(12)	1.773(7)
B(1)–B(3)	1.787(12)	1.781(5)	B(3′)–B(4′)	1.748(11)	1.774(6)
B(1)–B(8′)	1.895(11)	1.916(6)	B(4′)–B(8′)	1.788(11)	1.753(6)
B(1)–B(4′)	2.016(11)	1.987(6)	B(5′)–B(11′)	1.761(13)	1.744(6)
B(2)–B(3)	1.733(11)	1.784(5)	B(5′)–B(6′)	1.764(11)	1.765(6)
B(2)–B(11′)	1.906(12)	1.891(5)	B(6′)–B(11′)	1.714(13)	1.746(6)
B(2)–B(5′)	1.985(11)	2.042(5)	B(6′)–B(12′)	1.732(12)	1.775(6)
B(1′)–B(4′)	1.755(12)	1.769(7)	B(7′)–B(8′)	1.824(12)	1.845(7)
B(1′)–B(5′)	1.725(11)	1.768(6)	B(7′)–B(12′)	1.877(13)	1.915(7)
B(1′)–B(3′)	1.789(13)	1.799(6)	B(11′)–B(12′)	1.789(14)	1.876(6)
Bond angels					
O(1)–C(1′)–C(2′)		109.2(4)	B(6′)–B(1′)–B(3′)	109.7(6)	111.2(3)
B(5′)–O(1)–C(1′)		122.8(3)	B(4′)–B(1′)–B(3′)	59.1(5)	59.6(3)
B(4′)–O(1)–H(1A)	109.5		O(1)–B(4′)–B(3′)	119.1(6)	121.7(3)
B(2)–B(1)–B(3)	58.5(5)	60.5(2)	O(1)–B(4′)–B(1′)	117.1(6)	
B(2)–B(1)–B(8′)	117.1(6)	118.7(3)	O(1)–B(5′)–B(6′)		121.9(3)
B(3)–B(1)–B(8′)	104.3(5)	103.0(3)	O(1)–B(4′)–B(8′)	123.7(6)	106.3(3)
B(5)–B(1)–B(8′)	134.3(6)	131.6(3)	O(1)–B(5′)–B(1′)		120.1(3)
B(4)–B(1)–B(8′)	112.1(5)	108.8(3)	O(1)–B(4′)–B(1)	109.6(5)	
B(6)–B(1)–B(8′)	142.1(6)	141.3(3)	B(3′)–B(4′)–B(8′)	58.7(5)	58.8(3)
B(6)–B(1)–B(4′)	87.8(5)	88.0(2)	B(1′)–B(4′)–B(8′)	108.6(6)	109.5(3)
B(2)–B(1)–B(4′)	95.6(5)	96.8(3)	B(3′)–B(4′)–B(1)	115.2(5)	116.9(3)
B(3)–B(1)–B(4′)	137.0(6)	136.6(3)	B(8′)–B(4′)–B(1)	59.4(4)	61.3(2)
B(5)–B(1)–B(4′)	116.2(5)	115.7(3)	B(1′)–B(4′)–B(1)	126.8(6)	128.4(3)
B(4)–B(1)–B(4′)	158.1(6)	154.0(3)	B(3′)–B(4′)–B(1′)	61.4(5)	61.0(3)
B(8′)–B(1)–B(4′)	54.3(4)	53.3(2)	B(1′)–B(5′)–B(11′)	109.1(6)	109.9(3)
B(3)–B(2)–B(11′)	103.6(6)	103.4(3)	B(1′)–B(5′)–B(6′)	60.3(5)	61.6(3)
B(1)–B(2)–B(11′)	118.3(6)	118.1(3)	B(11′)–B(5′)–B(6′)	58.2(5)	59.7(2)
B(7)–B(2)–B(11′)	110.8(6)	110.3(3)	B(1′)–B(5′)–B(2)	128.7(6)	125.9(3)
B(6)–B(2)–B(11′)	142.5(7)	140.5(3)	B(11′)–B(5′)–B(2)	60.8(5)	59.3(2)
B(11)–B(2)–B(11′)	132.7(6)	132.3(3)	B(6′)–B(5′)–B(2)	115.5(6)	115.5(3)
B(3)–B(2)–B(5′)	138.6(6)	136.5(3)	B(3′)–B(8′)–B(4′)	59.5(5)	61.2(3)
B(1)–B(2)–B(5′)	96.5(6)	96.7(2)	B(3′)–B(8′)–B(7′)	60.3(5)	59.3(3)
B(7)–B(2)–B(5′)	154.1(6)	154.2(3)	B(4′)–B(8′)–B(7′)	105.7(6)	106.0(3)
B(6)–B(2)–B(5′)	88.7(5)	88.0(2)	B(3′)–B(8′)–B(1)	122.4(6)	123.0(3)
B(11)–B(2)–B(5′)	114.2(6)	115.4(3)	B(4′)–B(8′)–B(1)	66.3(4)	65.4(2)
B(11′)–B(2)–B(5′)	53.8(5)	52.5(2)	B(7′)–B(8′)–B(1)	122.8(6)	122.6(3)
B(1)–B(6)–B(2)	57.5(5)	58.4(2)	B(6′)–B(11′)–B(5′)	61.0(5)	60.7(2)
B(5′)–B(1′)–B(4′)	77.6(5)	78.2(2)	B(5′)–B(11′)–B(12′)	106.6(7)	105.9(3)
B(4′)–B(1′)–B(2′)	108.2(6)	108.0(3)	B(6′)–B(11′)–B(12′)	59.2(5)	58.5(2)
B(5′)–B(1′)–B(6′)	61.0(5)	59.1(2)	B(6′)–B(11′)–B(2)	122.4(7)	124.7(3)
B(5′)–B(1′)–B(2′)	108.0(6)	108.5(3)	B(5′)–B(11′)–B(2)	65.4(5)	68.2(2)
B(6′)–B(1′)–B(4′)	122.1(6)	121.2(3)	B(12′)–B(11′)–B(2)	122.8(7)	122.6(3)
B(5′)–B(1′)–B(3′)	121.2(6)	122.9(3)			

Attempts to grow crystals suitable for X-ray analysis of the $[NBzlEt_3]^+$ salts, **1** and **2**, led to data sets which were heavily disordered but the $[(\eta^5\text{-}C_5H_5)Fe(\eta^5\text{-}C_5H_4CH_2(Me)_3N)]^+$ salts **3** and **4** afforded crystals from which usable data sets were collected. The structures for **3** and **4** are illustrated in Figs. 1 and 2, respectively. The species are substituted in the 4′ or 5′ positions, which are equivalent and related by the mirror plane of the unsubstituted B_{22} cage. Two enantiomers of each are formed and in the case of the crystals for which we obtained structures, the (4′)-OH (**3**) and the (5′)-OEt (**4**) species were studied. The most significant difference between the structures of **3** and **4** and that of $[NBzlEt_3][N(PPh_3)_2][B_{22}H_{22}]$ [7b] is the B(4′)–B(5′) distance. This is the B–B bond adjacent to the conjunction between the two cages and one of the atoms bears the substituent. By examination of the two views in Fig. 1, we can demonstrate our visualization of **3** as consisting

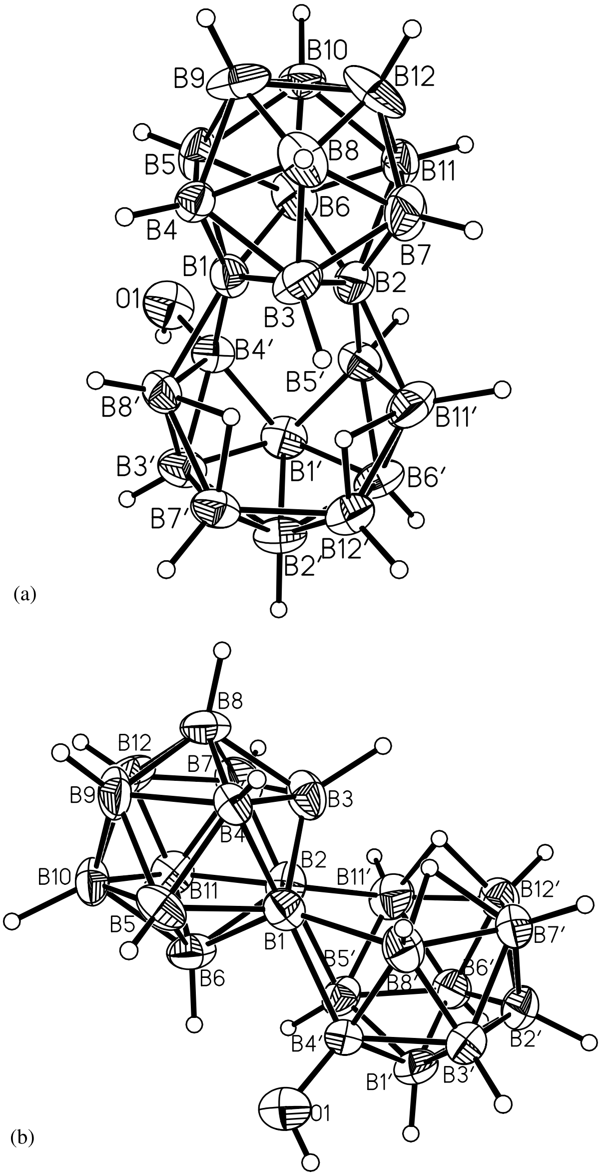

Fig. 1. (a) A view of the structure of the anion in **3** with 25% thermal ellipsoids. (b) An alternative view of **3**.

of a regular icosahedra *closo*-B_{12} cluster conjoined to a *nido*-B_{10} cluster. For such a system B(8′) and B(11′) in **3** are the "prow" positions in the *nido*-cluster and the two bridging H atoms are correctly positioned. The missing pair of bridging H atoms from the *nido*-$B_{10}H_{14}$ cluster would be in positions roughly equivalent to those of B(1) and B(2) in the B_{12} cage in **3**. Thus, the B(4′)–B(5′) axis is equivalent to the B(7′)–B(12′) axis in the *nido*-cluster, and these represent the "gunwale" positions of decaborane(14). The gunwale distance in *nido*-$B_{10}H_{14}$ is 1.973(4) Å [18] and in the unsubstituted $[NBzlEt_3][N(PPh_3)_2][B_{22}H_{22}]$ species, B(7′)–B(12′) is 1.88(1) Å [7b]. However the other "gunwale" distance in the latter, B(4′)-B(5′), is 2.09(1) Å; noticeably longer, and is the longest B–B distance in the anion. In the case of **3** and **4**, the B(4′)–B(5′) distances are such that they are not quite within realistic bond lengths at 2.180 and 2.23 Å, respectively. Thus, the structures in Figs. 1 and 2 are drawn without bonds between the two atoms and it appears that the pairs of atoms in the two species are not bonded. We presume that it is the influence of the substituent on the cage that accounts for this. It has been suggested previously that the presence of OH groups on a borane cage results in lengthening of the bond *trans* to the B–O bond. Thus, one can consider a formal addition of electron density to the borane framework. Such was suggested for the species [2,3-$\{(CH_3)_2C_2\}$-4,7-$(OH)_2$-10-Br-*closo*-B_9H_6] in which lengthening of the bonds *trans* to the B–OH axes rendered a species with effectively a *nido*-framework [19]. Similar substituent influences have been suggested before in borane cluster systems [20]. In the case of **3**, the B–B distance is 2.180 Å, longer by more than 0.3 Å than a normal B–B bond. The lengthening of the B(4′)–B(5′) distance in **4** from that for $[NBzlEt_3][N(PPh_3)_2][B_{22}H_{22}]$ is even greater; the distance being 2.230 Å. This is consistent with the effect of the lone pairs on O providing additional electron density to the cage. The inductive affect of the ethoxy group should magnify this effect if indeed this is the correct explanation, and apparently it does. There are other differences in the structures of **3** and **4** from that for $[NBzlEt_3][N(PPh_3)_2][B_{22}H_{22}]$, but none of the bond length differences are more than 0.1 Å. The longest bonded B–B distances in **3** and **4** are those at the conjunction of the two cages, B(1)–B(8′), B(1)–B(4′), B(2)–B(5′) and B(2)–B(11′). The analogous distances in the

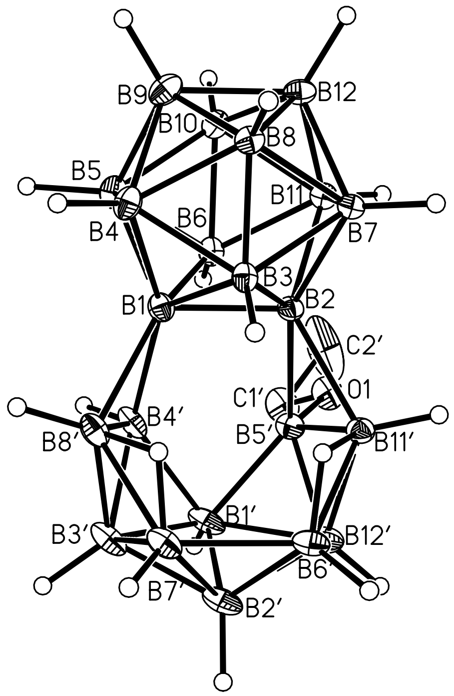

Fig. 2. A view of the structure of the anion in **4** with 25% thermal ellipsoids. Only the C atoms of the ethyl group are shown.

$[B_{22}H_{22}]^{2-}$ anion are also the longest B–B distances, except for B(4′)–B(5′).

The formation of derivatives of the $[B_{22}H_{22}]^{2-}$ anion is an important step towards further derivatization of this novel macropolyhedral borane, a development which is essential if such species are to be used in the future in medical applications, especially BNCT. Such derivatization would involve substitution of the H on OH, with some organic or biochemical group.

6. Supplementary material

Crystallographic data (excluding structure factors) for the structural analysis have been deposited with the Cambridge Crystallographic Data Centre, CCDC Nos. 205275 and 205274 for Compounds **3** and **4**, respectively. Copies of the information may be obtained free of charge from The Director, CCDC, 12 Union Road, Cambridge CB2 1EZ, UK (Fax: +44-1223-336033; e-mail: deposit@ccdc.cam.ac.uk or www: http://www.ccdc.cam.ac.uk).

Acknowledgements

We acknowledge the NSF (grant No. CHE-9727570), the Missouri Research Board and UM-St. Louis for research grants to L.B., and the NSF and the UM-St. Louis Center for Molecular Electronics and the Missouri Research Board for funds which help purchase the NMR, XRD and MS facilities.

References

[1] (a) L. Barton, T.P. Onak, Species containing more than 12 boron atoms, in: Gmelin Handbuch der Anorganischen Chemie, Erg-Werk, Borverbindungen 20, Vol. 54, 1979, pp. 240–304.;
(b) J. Bould, W. Clegg, S.J. Teat, L. Barton, N.P. Rath, M. Thornton-Pett, J.D. Kennedy, Inorg. Chim. Acta 289 (1999) 95;
(c) J. Bould, J.D. Kennedy, L. Barton, N.P. Rath, J. Chem. Soc. Chem. Commun. (1997) 2405.;
(d) H.-J. Yao, C.-H. Hu, J. Sun, R.-S. Jin, P.-J. Zheng, J. Bould, R. Greatrex, J.D. Kennedy, D.L. Ormsby, M. Thornton-Pett, Collect. Czech. Chem. Commun. 64 (1999) 927;
(e) M.F. Hawthorne, K. Shelly, F. Li, Chem. Commun. (2002) 547.

[2] (a) M.F. Hawthorne, in: W. Siebert (Ed.), Advances in Boron Chemistry, Royal Society of Chemistry, London, 1997, p. 261 (Special Publication);
(b) M.F. Hawthorne, in: M.G. Davidson, A.K. Hughes, T.B. Marder, K. Wade (Eds.), Contemporary Boron Chemistry, Royal Society of Chemistry, London, 2000, p. 197 (Special Publication).

[3] (a) M.F. Hawthorne, Mol. Med. Today 4 (1998) 174;
(b) A.H. Soloway, W. Tjarks, B. Barnum, F.G. Rong, R.F. Barth, I.M. Codogni, J.G. Wilson, Chem. Rev. 98 (1998) 1515;
(c) B. Larsson, J. Crawford, R. Weinreich (Eds.), Advances in Neutron Capture Therapy: Chemistry and Biology, Vol. 2, Elsevier, Amsterdam, 1997.;
(d) M.F. Hawthorne, A. Maderna, Chem. Rev. 99 (1999) 3421;
(e) M.F. Hawthorne, K. Shelly, R.J. Wiersema (Eds.), Proceedings of the Eighth International Symposium Frontiers in Neutron Capture Therapy, Vol. 1, 13–18 September 1998, Los Angeles, CA, 2001, 759 pp. and references therein.

[4] P. Kaszynski, ACS Symp. Ser. 798 (2001) 68.

[5] A.R. Pitochelli, M.F. Hawthorne, J. Am. Chem. Soc. 82 (1960) 3228.

[6] A.R. Pitochelli, M.F. Hawthorne, J. Am. Chem. Soc. 84 (1962) 3218.

[7] (a) N.S. Hosmane, A. Franken, G. Zhang, R.R. Srivastava, R.Y. Smith, B.F. Spielvogel, Main Group Met. Chem. 21 (1998) 319;
(b) O. Volkov, W. Dirk, U. Englert, P. Paetzold, Z. Anorg. Allg. Chem. 625 (1999) 1193.

[8] (a) T. Jelinek, J.D. Kennedy, B. Stibr, J. Chem. Soc. Chem. Commun. (1994) 1415.;
(b) J. Bould, W. Clegg, J.D. Kennedy, S.J. Teat, M. Thornton-Pett, J. Chem. Soc. Dalton. Trans. (1997) 2005.;
(c) J. Bould, S.A. Barrett, L. Barton, N.P. Rath, J.D. Kennedy, Inorg. Chem. Commun. 1 (1998) 365.

[9] (a) I.B. Sivaev, V.I. Bregadze, S. Sjoberg, in: M.G. Davidson, A.K. Hughes, T.B. Marder, K. Wade (Eds.), Contemporary Boron Chemistry, Royal Society of Chemistry, London, 2000, p. 135 (Special Publication);
(b) J. Bould, U. Doerfler, W. Clegg, S.J. Teat, M. Thornton-Pett, J.D. Kennedy, Chem. Commun. (2001) 1788.

[10] (a) T. Peymann, C.B. Knobler, M.F. Hawthorne, J. Am. Chem. Soc. 121 (1999) 5601;
(b) T. Peymann, C.B. Knobler, S.I. Khan, M.F. Hawthorne, J. Am. Chem. Soc. 123 (2001) 2182;
(c) T. Peymann, C.B. Knobler, S.I. Khan, M.F. Hawthorne, Inorg. Chem. 40 (2001) 1291;
(d) A. Herzog, R.P. Callahan, C.L.B. Macdonald, V.M. Lynch, M.F. Hawthorne, R.J. Lagow, Angew. Chem. Int. Ed. Engl. 40 (2001) 2121;
(e) A. Maderna, C.B. Knobler, M.F. Hawthorne, Angew. Chem. Int. Ed. Engl. 40 (2001) 1662;
(f) T. Peymann, C.B. Knober, S.I. Khan, M.F. Hawthorne, Angew. Chem. Int. Ed. Engl. 40 (2001) 1664;
(g) J. Thomas, M.F. Hawthorne, Chem. Commun. (2001) 1884.;
(h) A. Herzog, C.B. Knobler, S.I. Khan, M.F. Hawthorne, J. Am. Chem. Soc. 123 (2001) 12791.

[11] (a) R.J. Wiersema, R.L. Middaugh, J. Am. Chem. Soc. 89 (1967) 5078;
(b) R.J. Wiersema, R.L. Middaugh, Inorg. Chem. 8 (1969) 2074;
(c) R.J. Wiersema, R.L. Middaugh, J. Am. Chem. Soc. 92 (1970) 223.

[12] R. Bechtold, A. Kaczmarczyk, J. Am. Chem. Soc. 96 (1974) 5953.

[13] Bruker Analytical X-ray, Madison, WI, 2001.

[14] R.H. Blessing, Acta Crystallogr. A 51 (1995) 33.

[15] G.M. Sheldrick, Bruker Analytical X-ray Division, Madison, WI, 2001.

[16] D.F. Gaines, C.K. Nelson, G.A. Steehler, J. Am. Chem. Soc. 106 (1984) 7266.

[17] J. Bould, R. Greatrex, J.D. Kennedy, D. Ormsby, M. Londesborough, K.L.F. Callaghan, M. Thornton-Pett, T.R. Spalding, S.J. Teat, W. Clegg, H. Fang, N.P. Rath, L. Barton, J. Am. Chem. Soc. 124 (2002) 7229.

[18] A. Tippe, W.C. Hamilton, Inorg. Chem. 8 (1969) 464.

[19] M.E. Leonowicz, F.R. Scholer, Inorg. Chem. 19 (1980) 122.

[20] M.A. Fox, A.K. Hughes, J.M. Malget, J. Chem. Soc. Dalton Trans. (2002) 3505.